

# Rotational Evolution of Protoneutron Stars

Yefei Yuan<sup>1,2</sup> and Jeremy S. Heyl<sup>2,3</sup>

## ABSTRACT

We study the rotational evolution of a protoneutron star with hyperons and nucleons or solely nucleons in its core due to the escape of the trapped neutrinos. It is found that at the early stage of its evolution, the stellar crust contracts significantly, consequently the star spins up. At the late stage, a the protoneutron star with hyperons, it keeps shrinking and spinning up till all the trapped neutrinos escape. Consequently, the distribution of the stellar initial spin periods is skewed toward shorter periods. For a protoneutron star with only nucleons, the expansion of its core dominates, and the stellar rotation slows down. After the neutrinos escape, the range of the spin periods is narrower than the initial one, but the distribution is still nearly uniform. If the hyperonic star is metastable, its rotational frequency accelerates distinguishedly before it collapses to a black hole.

*Subject headings:* dense matter — stars: evolution, neutron, rotation

## 1. Introduction

A neutron star (NS) is born after the iron core collapse of a massive progenitor star ( $> 8M_{\odot}$ ) which exhausts its nuclear fuel. The birth of the neutron star often results in a Type-II supernova explosion (Burrows 2000). Immediately after its birth, the neutron star is hot and lepton-rich because the core is opaque to neutrinos. This young object is called a protoneutron star (PNS). As compared to the neutrino-free case (*i.e.* the cold neutron star), the trapped neutrinos significantly change the chemical equilibria between baryons and leptons, the fractions of all the compositions, and the equation of state (EOS).

---

<sup>1</sup>Center for Astrophysics, University of Science and Technology of China, Hefei, Anhui 230026, P.R. China; yfyuan@ustc.edu.cn

<sup>2</sup>Harvard-Smithsonian Center for Astrophysics, Cambridge, MA 02138; yyuan@cfa.harvard.edu; jhey1@cfa.harvard.edu

<sup>3</sup>Chandra Fellow

Therefore, the Kelvin-Helmholtz epoch of the evolution of the PNS, during which the PNS changes from a hot and lepton-rich compact star to a cold and neutrino-free one, is the most important evolutionary stage of the PNS. The time scale of the Kelvin-Helmholtz epoch completely depends on the neutrino interactions in the hot and dense matter (Reddy et al. 1998). Namely the diffusion time scale of the trapped neutrinos from the core to the outside is roughly several tens of seconds (Prakash et al. 1997). As pointed out in the literature, in principle, observations of supernova neutrinos may constrain the EOSs and the interior composition of neutron stars. (Prakash et al. 1995; Pons et al. 1999, 2001b,a).

The properties of PNSs which contain only ordinary nuclear matter have been investigated in detail by many authors (Takatsuka et al. 1994; Bombaci et al. 1995; Prakash et al. 1997; Hashimoto et al. 1994; Goussard et al. 1997, 1998; Strobel et al. 1999; Sumiyoshi et al. 1999). Because of the uncertainties of the composition of the matter in the interior of neutron stars, the effects of some exotic states, such as hyperonic matter (Prakash et al. 1997; Pons et al. 1999), quark matter (Pons et al. 2001b), kaon condensation (Pons et al. 2001a) and the quark-hadron phase transition (Prakash et al. 1995), on the evolution of PNSs have also been explored. Because the trapped neutrinos increase the chemical potential of electrons, the common consequence of the inclusion of the possible exotic states which contain negatively charged components in the PNS is the existence of a metastable star, the mass of which is larger than the maximum mass for a cold neutrino-free neutron star. Inevitably, the metastable PNS will collapse to a black hole at some time during the Kelvin-Helmholtz epoch. Meanwhile, the neutrino signal from the PNS will cease suddenly, because the time scale of the collapse is on the order the free-fall time which is much shorter than the evolutionary time scale of the PNS.

As the trapped neutrinos escape, the global structure of the PNS changes, especially the momentum of inertia which affects the stellar rotational frequency dramatically. Our key assumption is that Kelvin-Helmholtz timescale over which the neutrinos escape ( $\sim 10$  s) is much longer than the dynamical timescale of the PNS ( $\sim 1$  ms); therefore, the protoneutron star evolves through a series of hydrostatic equilibria with successively smaller neutrino fractions. In this work, we investigate the stellar global properties as a function of the number density of the trapped electron neutrinos. Especially, we contrast the rotational evolution of hyperonic PNSs with ordinary PNSs. The evolutionary behavior of a PNS in whose core the other possible exotic states exist is qualitatively similar to the results for the hyperonic star. In order to describe the hyperonic matter with trapped neutrinos, the relativistic mean field theory (RMFT) has been generally applied (Walecka 1974; Chin 1977; Serot 1979; Serot & Walecka 1986; Müller & Serot 1996; Prakash et al. 1997; Yuan & Zhang 1999; Glendenning 2000). The potential model is also used sometimes (Prakash et al. 1997). Recently, the potential model with the Bruecker-Bethe-Goldstone many-body theory at zero

temperature was employed to model the hyperonic matter with trapped neutrinos, and to investigate the global properties of the PNSs. As expected, the qualitative results which have been obtained in the both models are very similar (Vidana et al. 2003). The previous works have indicated that the effect of the trapped neutrinos dominates over that of temperature on the internal composition and EOS (Prakash et al. 1997). Thus, for simplicity, we use the RMFT to describe the dense nuclear matter with hyperons at zero temperature, and explore the response of the rotational frequency to the escape of the neutrinos.

After its birth, the neutron star generally spins fast initially, even near to the Keplerian angular velocity,  $\Omega_K$  (Fryer & Heger 2000). Stellar rotation is essential for the generation of the magnetic field (*e.g.* Thompson & Duncan 1993) and affects the global properties of the PNS significantly (Akiyama et al. 2003). In order to deal with the rotation of a rapidly rotating neutron star, a fully general relativistic method should be used. Several independent techniques exist in the literature (Stergioulas 1998). Our calculation is based on the Stergioulas & Friedman’s KEH codes (Komatsu et al. 1989a,b), which is available as a public domain code (Stergioulas & Friedman 1995).

This paper is organized as follows. A brief description of the RMFT for dense matter with hyperons, the microscopic properties of dense matter in  $\beta$ -equilibrium, and the global properties of the non-rotating and rapidly rotating PNSs are given in § 2. In § 3, the numerical results of the evolution of the rotational frequency is presented. The results and discussions will be given in § 4.

## 2. Equations of state for protoneutron stars

### 2.1. Description of the dense matter

In the framework of relativistic field theory, the interaction between nucleons and hyperons is mediated by the exchange of three meson fields,  $\sigma$ ,  $\omega$ , and  $\rho$  mesons. The coupling constants and meson masses can be algebraically related to the bulk properties of the symmetric nuclear matter (Glendenning 2000). The Lagrangian of the hadrons is given by,

$$\begin{aligned}
 \mathcal{L} = & \sum_i \bar{\psi}_i \left[ i\gamma_\mu \left( \partial^\mu + ig_{\omega i} \omega^\mu + i\frac{g_{\rho i}}{2} \boldsymbol{\tau} \cdot \boldsymbol{\rho}^\mu \right) - (m_i - g_{\sigma i} \sigma) \right] \psi_i \\
 & + \frac{1}{2} (\partial_\mu \sigma \partial^\mu \sigma - m_\sigma^2 \sigma^2) - U(\sigma) \\
 & - \frac{1}{4} \omega_{\mu\nu} \omega^{\mu\nu} + \frac{1}{2} m_\omega^2 \omega_\mu \omega^\mu \\
 & - \frac{1}{4} \boldsymbol{\rho}_{\mu\nu} \cdot \boldsymbol{\rho}^{\mu\nu} + \frac{1}{2} m_\rho^2 \boldsymbol{\rho}_\mu \cdot \boldsymbol{\rho}^\mu,
 \end{aligned} \tag{1}$$

where,

$$\omega_{\mu\nu} = \partial_\mu \omega_\nu - \partial_\nu \omega_\mu, \quad (2)$$

$$\boldsymbol{\rho}_{\mu\nu} = \partial_\mu \boldsymbol{\rho}_\nu - \partial_\nu \boldsymbol{\rho}_\mu + g_{\rho m} \boldsymbol{\rho}_\mu \times \boldsymbol{\rho}_\nu. \quad (3)$$

Throughout this paper we will use the set of natural units where  $\hbar = c = 1$  unless noted otherwise. Here  $\psi_i$ ,  $\sigma$ ,  $\omega$ , and  $\boldsymbol{\rho}$  denote the fields of the baryon of species  $i$  ( $i = n, p, \Lambda, \Sigma^-, \Sigma^0, \Sigma^+, \Xi^-, \Xi^0$ ), the mesons  $\sigma$ ,  $\omega$ , and  $\rho$  with the masses of  $m_i$ ,  $m_\sigma$ ,  $m_\omega$ ,  $m_\rho$ , respectively. The constants  $g_{\sigma i}$ ,  $g_{\omega i}$ ,  $g_{\rho i}$  are coupling constants for interactions between mesons and baryons.  $\boldsymbol{\tau} = (\tau_1, \tau_2, \tau_3)$  denotes the  $2 \times 2$  Pauli isospin matrices and the dot and cross products are calculated over isospin space. The potential of the self-interaction of the scalar field which reads,

$$U(\sigma) = \frac{1}{3} b m_n (g_{\sigma n} \sigma)^3 + \frac{1}{4} c (g_{\sigma n} \sigma)^4, \quad (4)$$

is introduced to produce reasonable incompressibility of nuclear matter (Boguta & Bodmer 1977). Here the coefficients  $b$  and  $c$  denote self-coupling constants for the  $\sigma$  meson field.

The dynamical equations of nucleons and mesons can be derived from the above Lagrangian. Generally, these equations are coupled. Applying the RMFT approximation (Walecka 1974), the dynamical equations are decoupled, they are,

$$\mu_i = g_{\omega i} \omega_0 + g_{\rho i} \rho_{03} I_{3i} + \sqrt{k^2 + m_i^{*2}}, \quad (5)$$

$$m_\sigma^2 \sigma = g_{\sigma i} n_{si} - \frac{\partial U(\sigma)}{\partial \sigma}, \quad (6)$$

$$\omega_0 = \sum_i \frac{g_{\omega i}}{m_\omega^2} n_i, \quad (7)$$

$$\rho_{03} = \sum_i \frac{g_{\rho i}}{m_\rho^2} I_{3i} n_i. \quad (8)$$

Here,  $\mu_i$  is the chemical potentials of baryons,  $I_{3i}$  is the third component of isospin for the baryons, and  $m_i^* = m_i - g_{\sigma i} \sigma$  are the effective masses of baryons. Finally, the scalar density  $n_{si} \equiv \langle \bar{\psi} \psi \rangle$  is defined as

$$n_{si} = \frac{2}{\pi^2} \int_0^{k_i^F} \frac{m_i^*}{\sqrt{k^2 + (m_i^*)^2}} k^2 dk, \quad (9)$$

where  $k_i^F$  are the Fermi momenta of baryons. The condition of chemical equilibrium between baryons and leptons is given by,

$$\mu_i = b_i \mu_n - q_i \tilde{\mu}_l, \quad (10)$$

where  $b_i$  is the baryon number of particle  $i$  and  $q_i$  is its charge. For the neutrino-free case,  $\tilde{\mu}_l = \mu_l$ , for the trapped-neutrino case,  $\tilde{\mu}_l = \mu_l - \mu_{\nu_l}$ . Here  $\mu_l$  ( $l = e^-, \mu^-$ ) are the chemical

potentials of the leptons. Because neutrinos are trapped, the lepton number per baryon  $Y_{L_l}$  of each flavor must be conserved on dynamical time scales,

$$Y_{L_l} = Y_l + Y_{\nu_l} = \text{constant}. \quad (11)$$

Studies of the gravitational collapse calculations of the core of a massive star indicate that  $Y_{L_e} \simeq 0.4$  (Prakash et al. 1997). In addition, because no muons appear when neutrinos become trapped,  $Y_{L_\mu} = 0$ . During the Kelvin-Helmholtz epoch,  $Y_{\nu_e}$  changes from its initial value to zero. Therefore, if the chemical potential of neutrons and electrons are known, the fields of the mesons  $\sigma$ ,  $\omega$ , and  $\rho$  can be solved numerically, and then the momenta of all the baryons can be determined at the same time. Given the baryon number density  $n_B$ , the additional condition, charge neutrality, is needed to determine  $\mu_n$  and  $\mu_e$  self-consistently.

According to the standard procedure of RMFT theory (Walecka 1974), the energy density and the pressure of the baryons can be obtained,

$$\epsilon_B = \frac{1}{2}m_\sigma^2\sigma^2 + \frac{1}{2}m_\omega^2\omega_0^2 + \frac{1}{2}m_\rho^2\rho_{03}^2 + \sum_i \frac{1}{\pi^2} \int_0^{p_i^F} \sqrt{p^2 + m_i^*} p^2 dp, \quad (12)$$

$$p_B = -\frac{1}{2}m_\sigma^2\sigma^2 + \frac{1}{2}m_\omega^2\omega_0^2 + \frac{1}{2}m_\rho^2\rho_{03}^2 + \sum_i \frac{1}{\pi^2} \int_0^{p_i^F} \frac{p^4 dp}{\sqrt{p^2 + m_i^*}}. \quad (13)$$

The coupling constants  $g_{\sigma N}$ ,  $g_{\omega N}$ ,  $g_{\rho N}$ ,  $b$ ,  $c$  ( $N = n, p$ ) in RMFT are algebraically related to the bulk properties of symmetric nuclear matter at saturation density. In our calculation, we choose the so-called GM1 set (Glendenning & Moszkowski 1991),

$$\left(\frac{g_{\sigma N}}{m_\sigma}\right)^2 = 11.79, \quad \left(\frac{g_{\omega N}}{m_\omega}\right)^2 = 7.149, \quad \left(\frac{g_{\rho N}}{m_\rho}\right)^2 = 4.411, \quad b = 2.947 \times 10^{-3}, \quad c = -1.07 \times 10^{-3}, \quad (14)$$

from which the nuclear properties arise as follows: the saturation density, effective mass of nuclear, incompressibility, and binding energy per nucleon are  $n_0 = 0.153 \text{ fm}^{-3}$ ,  $m^* = 0.7$ ,  $K = 300 \text{ MeV}$ , and  $B/A = -16.3 \text{ MeV}$ .

At the saturation density, the bulk properties are independent of the hyperon couplings which could be determined by reproducing the binding of the  $\Lambda$  hyperon in nuclear matter (Glendenning & Moszkowski 1991). It is assumed that all hyperons in the octet have the same coupling which are expressed in terms of nucleon couplings,

$$x_{\sigma H} = \frac{g_{\sigma H}}{g_{\sigma N}}, \quad x_{\omega H} = \frac{g_{\omega H}}{g_{\omega N}}, \quad x_{\rho H} = \frac{g_{\rho H}}{g_{\rho N}}. \quad (15)$$

In the GM1 set (Glendenning et al. 1997; Glendenning & Moszkowski 1991; Glendenning 2000),

$$x_{\sigma H} = 0.6, \quad x_{\omega H} = x_{\rho H} = 0.653. \quad (16)$$

## 2.2. The interior composition and the EOS

The evolution of the PNS with time should be investigated by solving the neutrino transport equations (Pons et al. 1999; Janka et al. 2003; Rampp & Janka 2002). Due to the escape of the neutrinos,  $Y_{\nu_e}$  decreases with time. Because our purpose in this work is to explore the rotational behavior of the PNS as the neutrinos escape, we study the rotational frequency and other interesting quantities as a function of  $Y_{\nu_e}$ . The ratio of the number fraction of electron neutrinos to its initial value is assumed to be a constant with baryon number density, for a given time. Because the density in the stellar core is almost constant, this is a good approximation. As the electron neutrinos escape, the muon neutrino appears due to the following reaction,

$$e^- \rightarrow \mu^- + \bar{\nu}_\mu + \nu_e \quad . \quad (17)$$

To describe the escape of the muon neutrinos, we assume that the ratio of the number of the escaped muon neutrinos to that of the muon neutrinos which should escape freely if the matter is transparent to neutrinos equals to  $Y_{\nu_e}/Y_{\nu_e}^i$ . Our calculations show the number density of muons is generally several orders of magnitude lower than that of electrons, so its effects on the EOS of PNS could be neglected, even though we have taken it into consideration.

Previous studies have shown that neutrinos are trapped above a density  $n_{\text{env}} \approx 6 \times 10^{-4} \text{ fm}^{-3}$  (Burrows et al. 1995; Strobel et al. 1999). Therefore, before the neutrinos escape, we set  $Y_{\text{Le}} = 0.4$  for densities above  $n_{\text{env}}$ . For the description of neutrino-free subnuclear matter, the FPS EOS (Lorenz et al. 1993) is chosen, which is smoothly matched to the EOS of nuclear matter described in RMFT. At low baryon number density ( $n_{\text{B}} < 0.1 \text{ fm}^{-3}$ ), the nucleons are non-relativistic, thus the pressure contributed by the trapped neutrinos and the relativistic electrons dominates. The EOS of subnuclear dense matter becomes much stiffer due to the trapped neutrinos (see Fig. 1).

The main effect of the neutrino trapping in the dense matter above nuclear density is that the fraction of electrons increases dramatically, regardless of the interior composition. Therefore, for a protoneutron star which contains only nucleons in its core, the fraction of protons is forced to increase in the same manner because of charge neutrality. Comparing to the neutrino-free case, the symmetry energy which is contributed by the  $\rho$  meson and linearly depends on the difference between the baryon number density of neutrons and protons, decreases significantly (see Eq. 8 and Eq. 12-13). Consequently, the EOS in the normal stellar core is softer with trapped neutrinos than without them. For hyperonic matter, the higher chemical potential of electrons that results from trapped neutrinos increases the critical baryon number density of the appearance of  $\Sigma^-$  particles. Because there are fewer species of baryons, the Fermi momenta of each species is larger, so the pressure of hyperonic matter with trapped neutrinos is larger than the pressure without neutrinos (see Fig. 2).

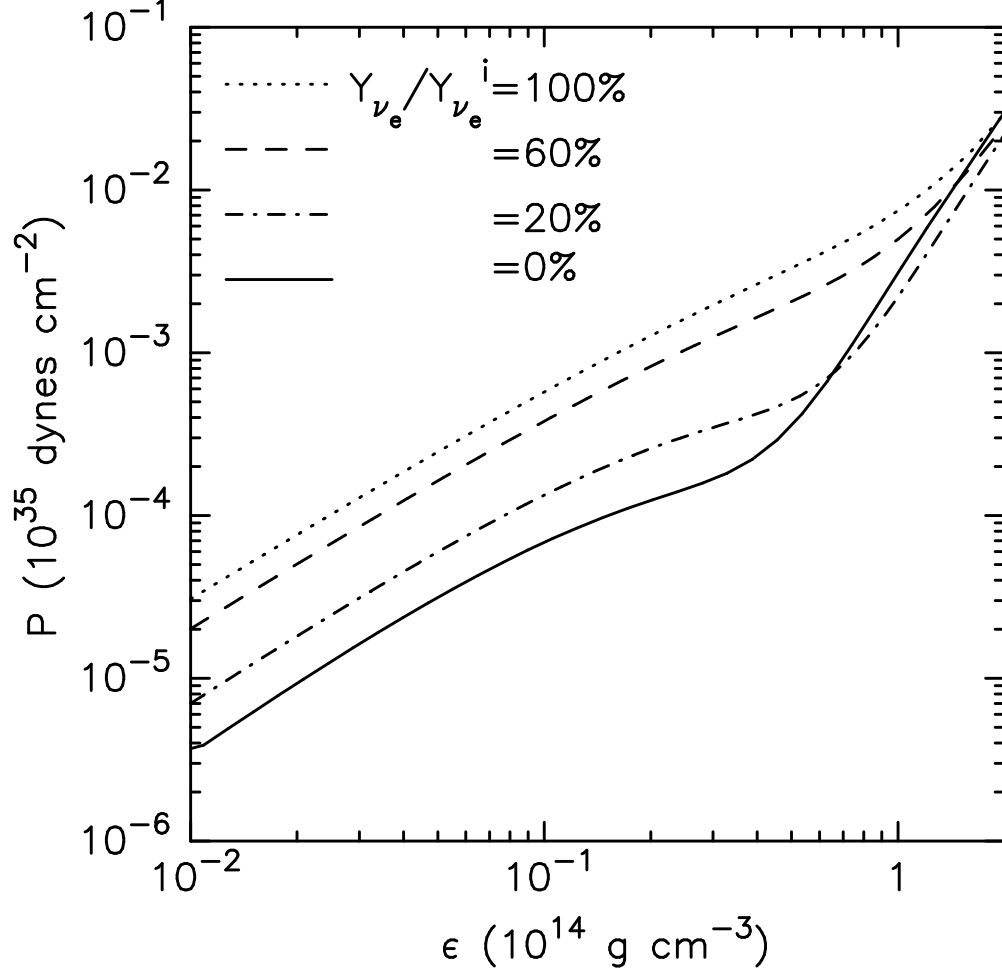


Fig. 1.— The pressure versus the energy density in the stellar envelope at different ratios of the fraction of trapped electron neutrinos to the initial value. Before the neutrinos escape,  $Y_{L_e} = 0.4$ ,  $Y_{L_\mu} = 0$ .

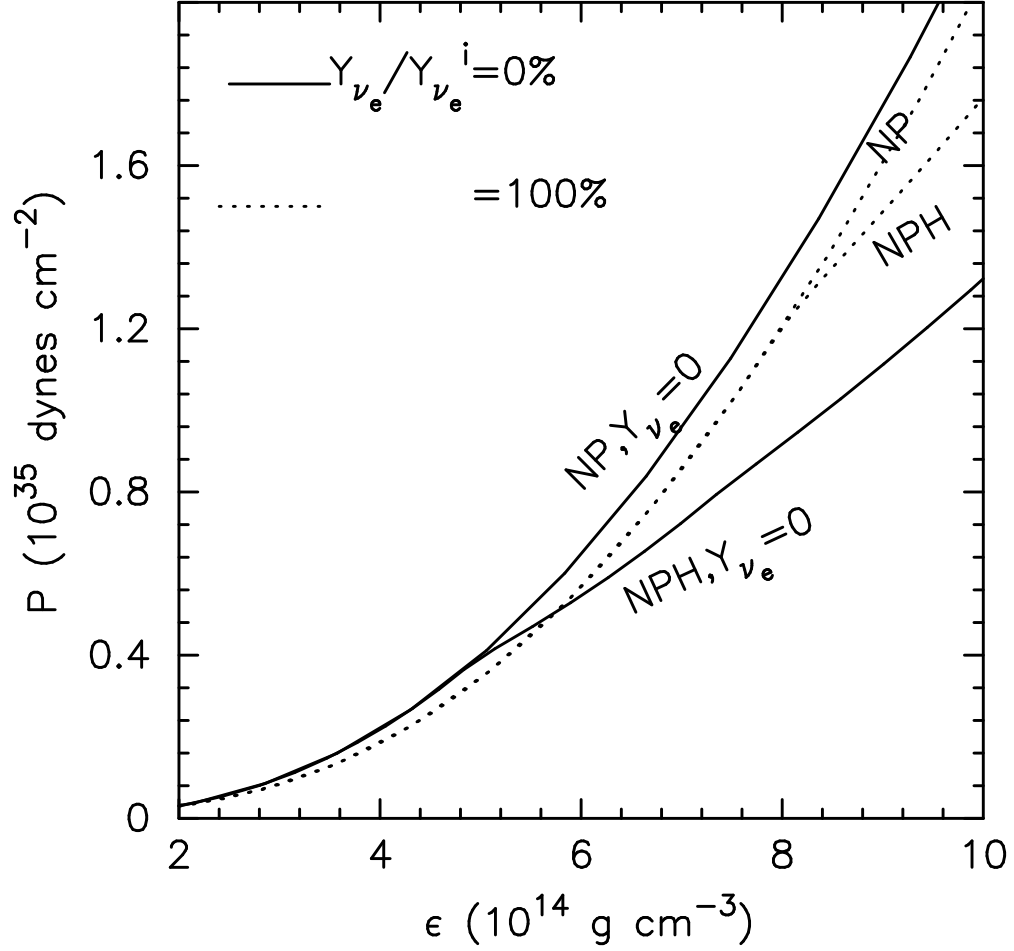


Fig. 2.— The comparison of the EOSs between the neutrino-trapped matter (dotted lines) and the neutrino-free matter (solid lines) in a stellar core which contains only nucleons (labeled as 'NP') and which contains hyperons as well (labeled as 'NPH').



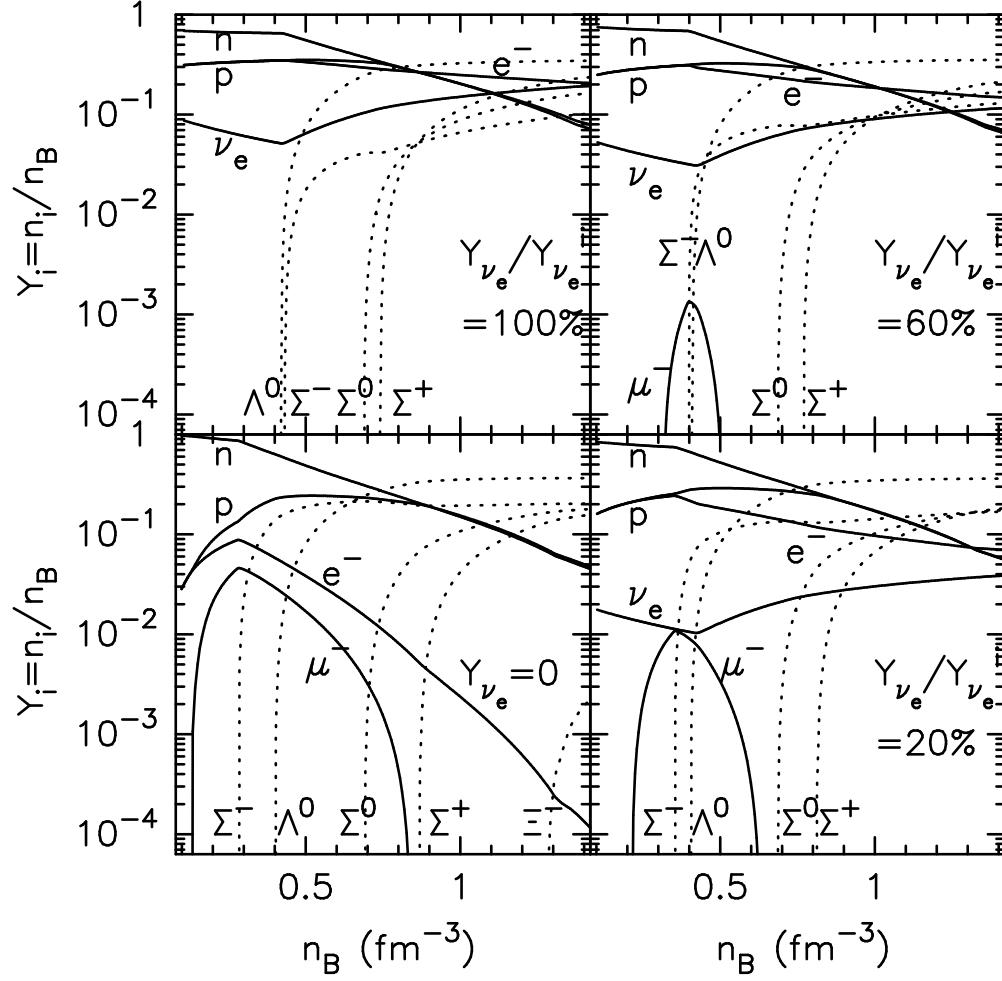


Fig. 3.— The relative compositions ( $Y_i$ ) as a function of the baryon number density ( $n_B$ ) at the different values of  $Y_{\nu_e}/Y_{\nu_e}^i$  in the hyperonic matter.

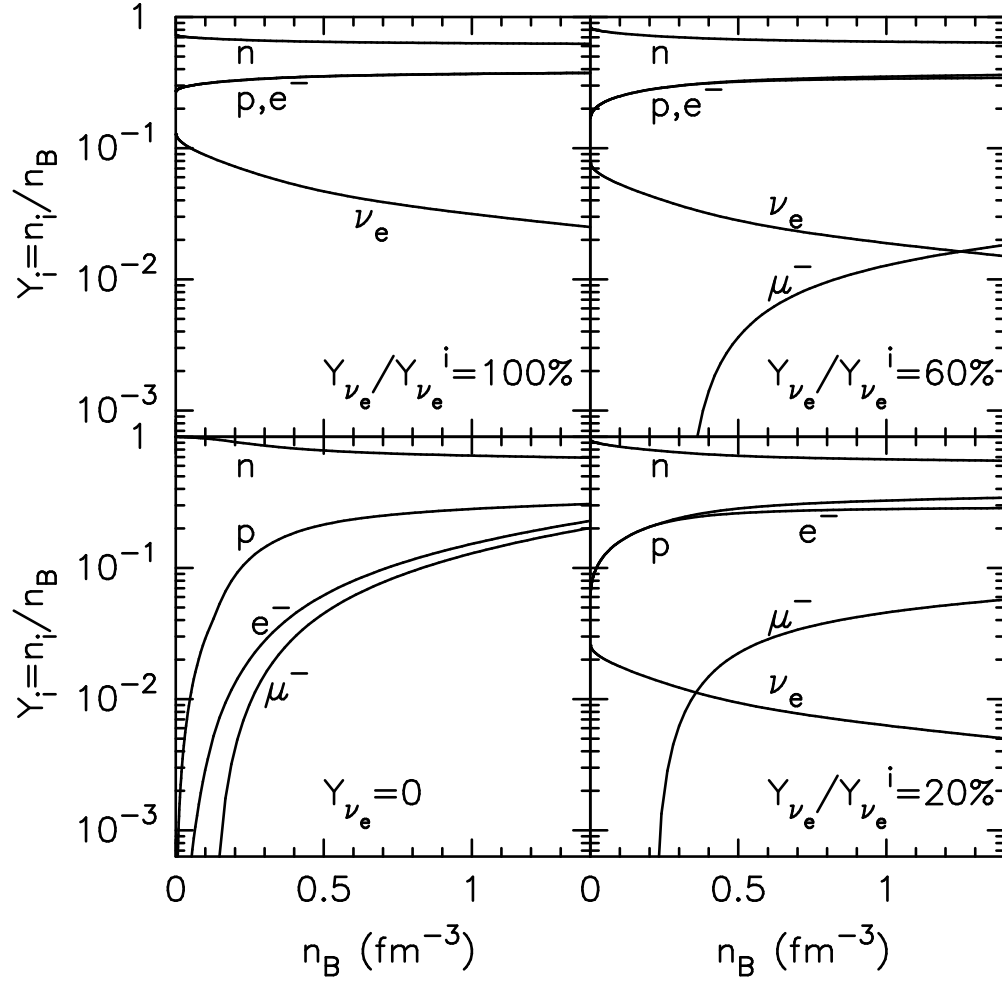


Fig. 4.— The same as Fig. 3, but for the normal nuclear matter which consists of nucleons.

Figure 3 shows the composition of matter in the stellar interior which contains hyperons. The subfigures in Fig. 3 are the results for  $Y_{\nu_e}/Y_{\nu_e}^i = 100\%, 60\%, 20\%, 0$ , respectively. As noticed in previous work, the neutrino trapping causes the following results: (1) muons do not appear; (2) the number density of electrons and protons increases significantly; (3) the onset of the negatively charged hyperons takes place at higher baryon number density, chargeless hyperons appear at nearly the same baryon number density, while the onset of positively charged hyperons occurs at lower density (see Fig. 3). The whole effect is that the EOS of the hyperonic matter becomes stiffer at high density. With the escape of the trapped neutrinos, muons begin to appear and  $\Sigma^-$  particles appear at lower density.

For the purpose of comparison, Fig. 4 shows the composition of the matter which includes only nucleons. As in the above case, the neutrino trapping suppresses the appearance of muons and increases the number density of electrons and protons.

The responses of the EOSs based on the hyperon model (NPH) and nucleon model (NP) as the neutrinos escape are shown in Fig. 5. In the NP model, as expected, the EOSs become more and more stiff as the neutrinos escape. The same occurs in the NPH model, below the critical density of the emergence of the hyperons. However, in the NPH model, at densities above the critical density, the EOSs become softer due to the appearance of the more and more additional components.

### 2.3. Properties of the non-rotating and rapidly rotating PNSs

In order to solve the Einstein field equations with the source terms, neutron-star matter is generally assumed to behave as a perfect fluid. For a static neutron star, the resulting equations are well known, the Tolman-Oppenheimer-Volkoff equations. It is complicated to deal with the rotation of a neutron star. If the stellar angular velocity  $\Omega$  is small compared to the critical value  $\Omega_0 = \sqrt{4\pi G \epsilon_c}$ , where  $\epsilon_c$  is the mass density at the center of the star, the perturbation theory developed by Hartle and Thorne is accurate enough (Hartle 1967; Hartle & Thorne 1968; Chubarian et al. 2000). Hartle’s original perturbation theory was improved by considering the effects of centrifugal stretching and frame dragging in an attempt to calculate the properties of a rapidly rotating neutron star with  $\Omega \sim \Omega_0$  (Glendenning 1992; Weber & Glendenning 1992). Nevertheless, the exact treatment of the rotation of a compact star should be done in full general relativity. Several reasonable assumptions are generally made, they are, the spacetime and the matter are stationary and axisymmetric, and the star uniformly rotates. Under these assumptions, the metric of the spacetime can be expressed by

$$ds^2 = e^{\gamma+\rho} dt^2 + e^{2\alpha} (dr^2 + r^2 d\theta^2) + e^{\gamma-\rho} r^2 \sin^2 \theta (d\phi - \omega dt)^2, \quad (18)$$

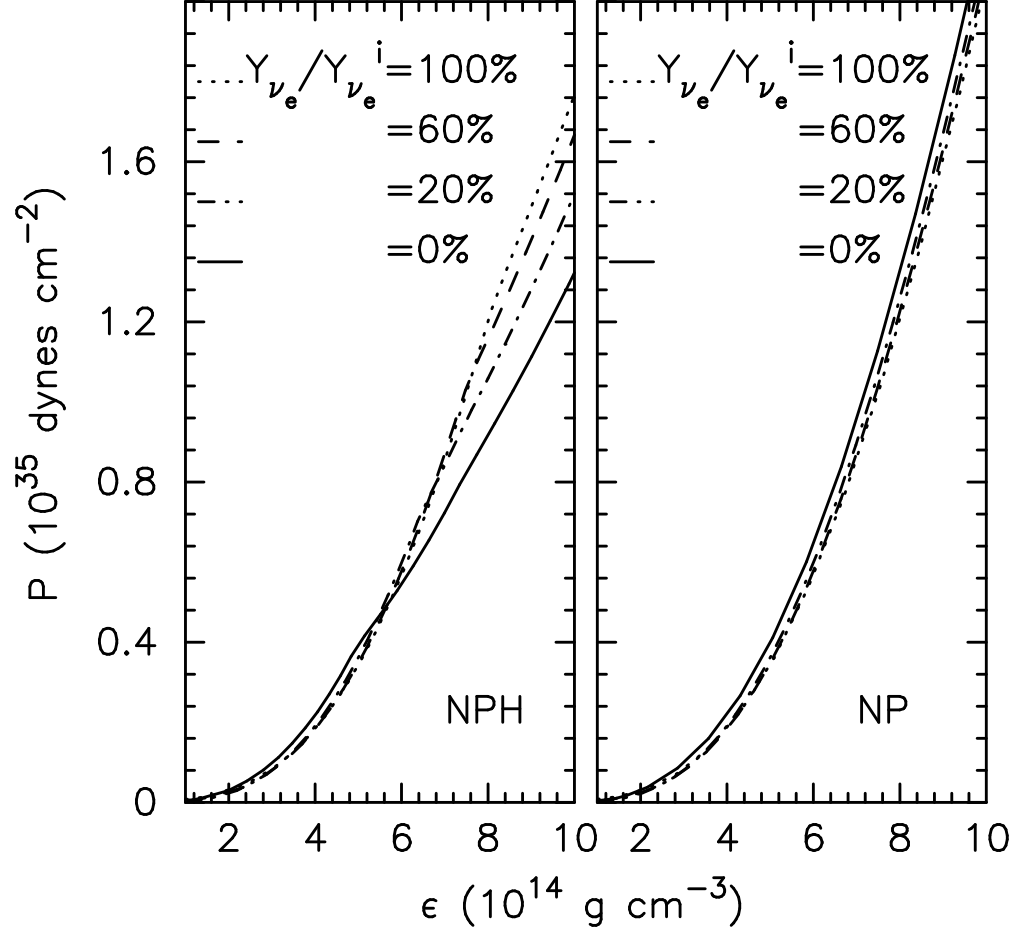


Fig. 5.— The change of the EOSs of the hyperonic matter (left panel), and the normal nuclear matter (right panel) due to the escape of the neutrinos.

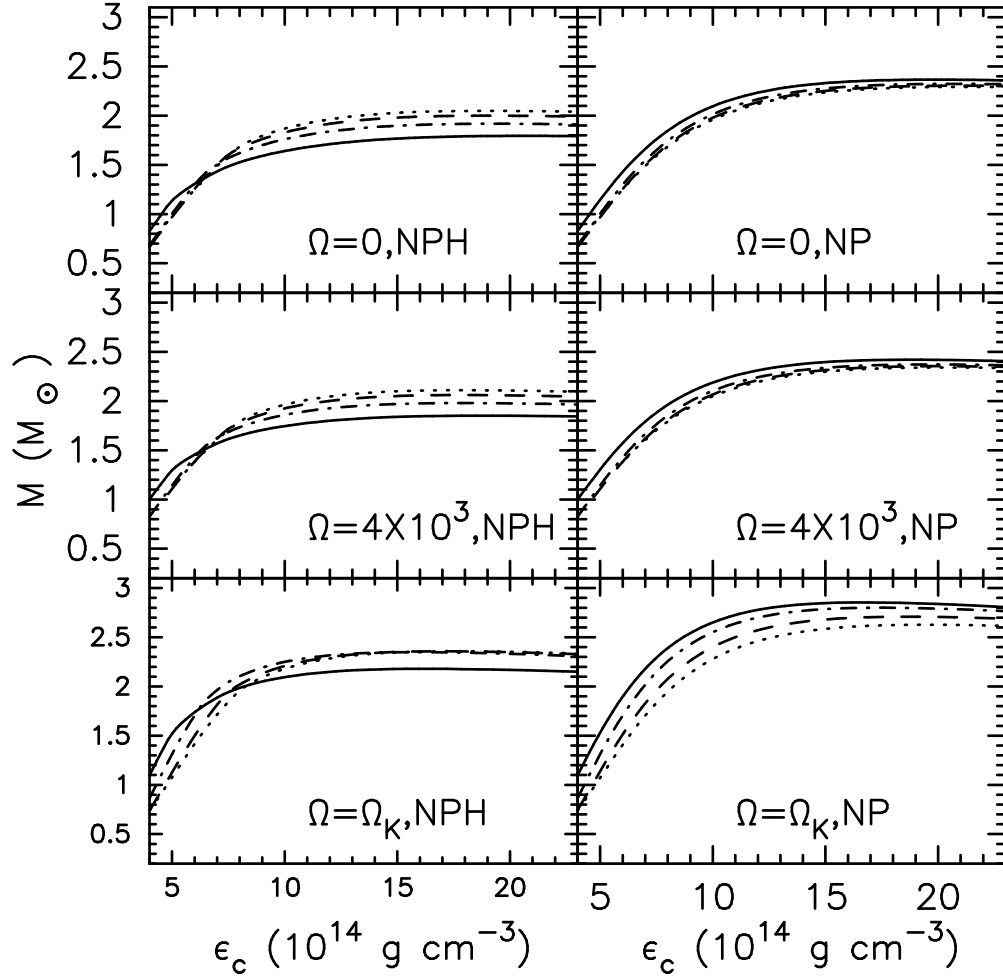


Fig. 6.— The gravitational mass  $M$  as a function of the central density at the different rotation frequencies  $\Omega = 0$ ,  $\Omega = 4 \times 10^3$ ,  $\Omega = \Omega_K$ . Left panels are the results for hyperonic matter, while right panels for the nuclear matter. The solutions traced by the various lines are the same as in Fig. 5, which represent the different values of  $Y_{\nu_e}/Y_{\nu_e}^i$ .

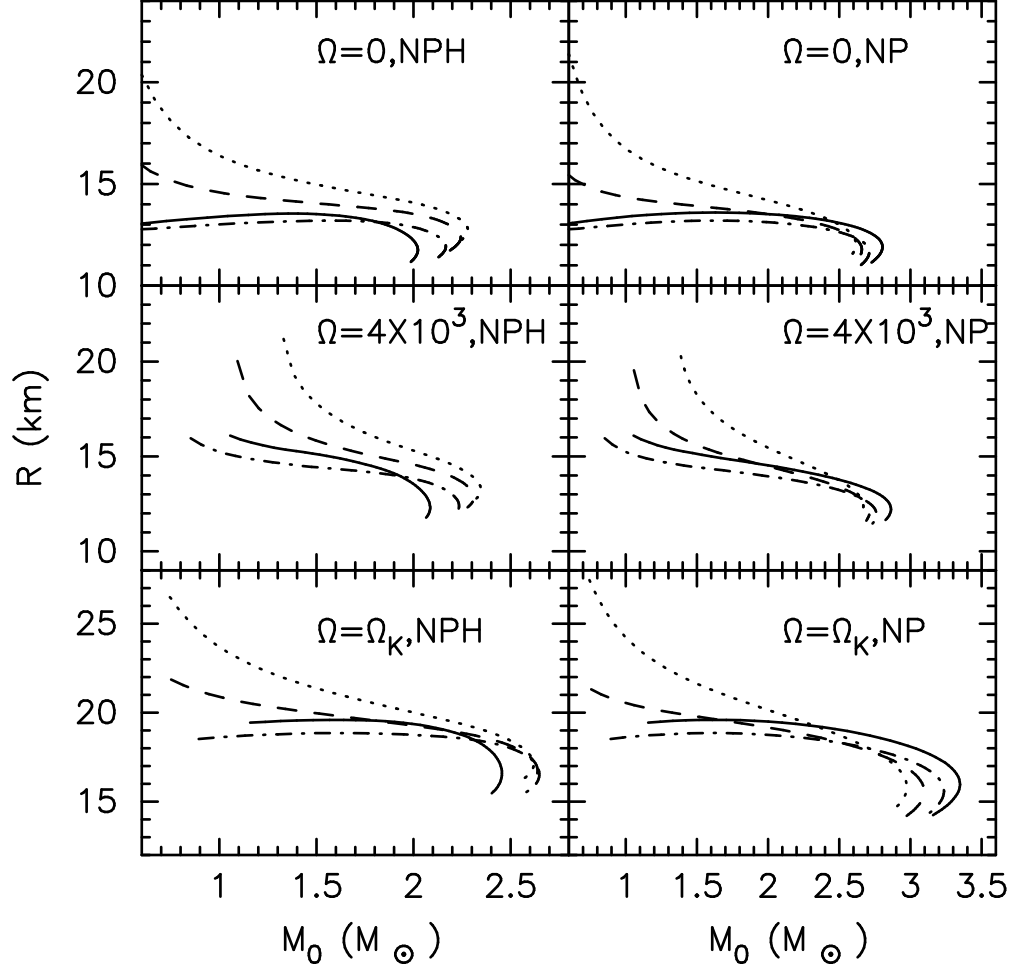


Fig. 7.— The stellar radii as a function of the baryonic mass. The solutions traced by the various lines are the same as in Fig. 5.

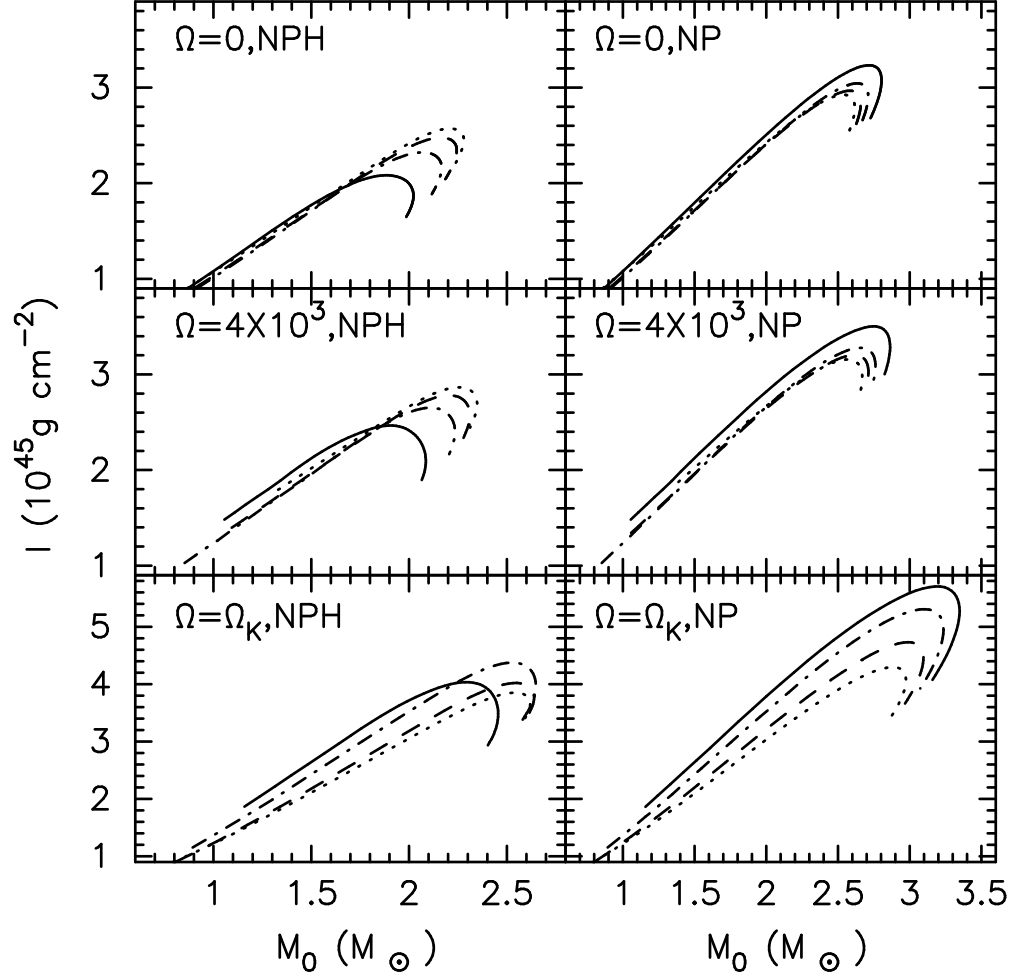


Fig. 8.— The stellar momenta of inertia as a function of the baryonic mass. The solutions traced by the various lines are the same as in Fig. 5.

where the metric potentials  $\gamma, \rho, \omega$  and  $\alpha$  are functions of  $r$  and  $\theta$  only. Several independent methods to numerically calculate the metric potentials exist. After solving the metric potentials, any coordinate-invariant physical quantity can be calculated.

Figures 6-8 show the global properties of the neutron stars. In Fig. 6, we plot the gravitational mass ( $M$ ) as a function of the central energy-density ( $\epsilon_c$ ) for PNSs with different fractions of trapped neutrinos  $Y_{\nu_e}/Y_{\nu_e}^i$  and with different rotational frequencies  $\Omega = 0$ ,  $\Omega = 4 \times 10^3$ , and  $\Omega = \Omega_K$  in both the NP and NPH model. As predicted in the previous works, the maximum mass of the static PNS decreases as the neutrinos escape in the NPH model, which results in the possible existence of a metastable star. In the NP model the maximum mass increases as the neutrinos escape. These results hold even when the PNS spins very rapidly.

Figures 7-8 show the radii and the moments of inertia as a function of the rest mass respectively. In the NP model, if the stellar rest mass  $M_0$  is near the maximum mass, the radii  $R$  and the moments of inertia  $I$  increase as the neutrinos escape, while decrease in the NPH model. Evidently, this behavior is dominated by the change of the EOSs in the stellar core. The trapped neutrinos always make the EOS in the crust stiffer (see Fig. 1) because of the dominance of the lepton pressure. When the initial mass is small, firstly, the PNS shrinks as the neutrino escape the crust, then begins to expand when the pressure of the  $\rho$  meson which determines the symmetry energy is comparable to that of the leptons.

Figure 8 show the moments of inertia as a function of the rest mass. In the NP model, if the stellar rest mass  $M_0$  is near the maximum mass, the moments of inertia  $I$  increase as the neutrinos escape, as the radii  $R$  do. In the NPH model, the moments of inertia decrease. When the initial mass is small, firstly,  $I$  decreases then increases while the neutrinos escape. The change in behavior is not as significant as what happens to the radii, because gravitational mass increases as the neutrinos escape the core. In some sense, this compensates the decrease of the radius.

### 3. Rotational evolution of protoneutron stars

As investigated in the above section, the global structure of the PNS changes in different ways as the neutrinos escape depending on whether hyperons exist in the core. This may affect the rotational evolution of the PNS. During the evolution of the PNS, the baryonic mass is fixed, if there is no accretion. Neglecting the loss of angular momentum due to the radiation of gravitational and electromagnetic waves, the loss of the total angular momentum of the PNS only results from the escaping of the neutrinos. To determine how the loss of



angular momentum carried away by the neutrinos affects the rotational evolution, we also assume that the neutrinos do not carry any angular momentum as they escape.

Figure 9 shows the stellar radii and moment of inertia as a function of neutrino fraction. For the NP model, the radii decrease first mainly because the EOSs of the subdense matter in the stellar crust becomes softer as the neutrinos escape. The radii then increase mainly because the EOS of the dense matter in the stellar core becomes stiffer, as contribution from symmetry energy increases. For the NPH model, the radii keep decreasing because both the decrease of the neutrino pressure and the appearance of more and more hyperons in the stellar core make the EOS softer. If  $M_0 = 1.5M_\odot$ , hyperonic matter does not appear in the stellar core at all. If  $M_0 = 2.2M_\odot$ , the PNS is metastable, and it collapses to a black hole at the end of the Kelvin-Helmholtz epoch. The evolution of the total moment of inertia is very similar to that of the radii.

Figure 10 shows how the rotational frequency changes as the neutrinos escape in the NPH and NP model. Early in the Kelvin-Helmholtz epoch, the PNS always spins up independent of the presence of hyperons, because as neutrinos escape the envelope, the PNS shrinks. The crustal EOS affects the rotational evolution of a protoneutron star significantly (Cheng et al. 2002). Later in the evolution, roughly speaking, for the NPH model, the PNS spins up with the EOS in the stellar core becoming softer; while for the NP model, the PNS spins down with the EOS in the stellar core becoming stiffer. For  $M = 2.0M_\odot$ , in the middle of the evolution, the NPH spins down for a short period. Even though the increased number of hyperons make the EOS softer, at the same time the fraction of the proton decreases, which makes the EOS stiffer. These two effects compete with each other, the spin down results from the increase of the symmetry energy. If the PNS is metastable, the star keeps spinning up significantly, and then collapses to a black hole at the end of its life. It is clearly shown in Fig. 10 that even though the escaped neutrinos carry away some of the angular momentum which decreases the rotational frequency of the PNS, the effect of the change of the global structure due to the escape of the neutrinos dominates the stellar rotational evolution.

The change of the rotational frequencies of the PNS after the neutrinos escape would change the initial distribution of the periods of neutron stars. Assuming the distribution at the beginning of the Kelvin-Helmholtz epoch is uniform between zero and the Keplerian frequency ( $\sim 5344s^{-1}$  for  $M_0 = 2.0M_\odot$ ), the new distribution is shown in Fig. 11. For PNSs without hyperons, the range of the periods is somewhat narrower than before, but roughly speaking, the distribution is still almost uniform. For the PNS with hyperons, a significant number of slowly rotating PNSs shift to higher spins; consequently, the presence of hyperonic matter at the center of neutron stars will skew the distribution of initial spin periods toward

shorter periods.

Figure 12 shows the evolution of the integrated flux of the escaped electron neutrinos. The total energy of the trapped electron neutrinos  $E_\nu^{\text{tot}}$  may be estimated as follows: the average baryon number density  $n_B \simeq M/(\frac{4}{3}\pi R^3 m_n)$ , the corresponding neutrino number density  $n_{\nu_e} = n_B Y_{\nu_e}$ , and the Fermi energy of the trapped neutrinos  $E_{\nu_e}^F = p_{\nu_e}^F = (6\pi^2 n_{\nu_e})^{1/3} \sim 0.2\text{GeV}$ , therefore,  $E_\nu^{\text{tot}}$  is given by,

$$E_{\nu_e}^{\text{tot}} \simeq \frac{3}{4} n_{\nu_e} E_{\nu_e}^F \times \frac{4}{3} \pi R^3 \simeq 2.12 \times 10^{-2} \left( \frac{M}{2.0 M_\odot} \right)^{4/3} \left( \frac{R}{1.5 \times 10^6 \text{cm}} \right)^{-1} \left( \frac{Y_{\nu_e}}{0.1} \right)^{4/3} M_\odot. \quad (19)$$

It is evident that the total neutrino flux is of the same order for the different initial masses. The flux of the electron neutrinos in both the NPH model and NP model is also similar, because the hyperons only appear at a higher density when neutrinos are trapped, which makes the hyperonic PNS and the normal PNS very similar.

#### 4. Conclusions and discussion

In this paper, we investigate the rotational evolution of protoneutron stars which contain only nucleons with that of PNSs which contain hyperonic matter at zero temperature in full general relativity. It is found that PNSs contract and spin up at the early stage of its evolution as the trapped neutrinos escape. During this stage the contribution of leptons to the pressure in the stellar crust dominates. This conclusion is independent of the interior composition. As the neutrinos continue to escape, the evolution of the PNS mainly depends on the changing behavior of the EOS of the dense matter in the stellar core; therefore, it differs in the two different models. A PNS which contains only nucleons stops contracting and begins to expand because the EOS becomes stiffer as neutrinos escape from the core. PNSs that contain hyperonic matter keep shrinking, and their spin frequency increases because the EOS becomes softer with the escape of the neutrinos. At the end of the evolution, for PNSs without hyperons, the range of the spin periods becomes a little bit narrower than the initial one. However, the shape of the distribution of the spin periods is very similar to that of the initial distribution. For PNSs with hyperons, the distribution of the initial spin periods is skewed significantly toward shorter periods. If a PNS is metastable, it keeps spinning up significantly on the neutrino diffusion timescale before it collapses to a black hole.

In addition to the hyperonic matter, other exotic states, such as quark matter, kaon condensation and others might exist in the stellar core. Because the neutrino trapping makes the onset of these exotic states which contain negatively charged particles take place at the higher baryon number density, a PNS with such an exotic composition spins up as

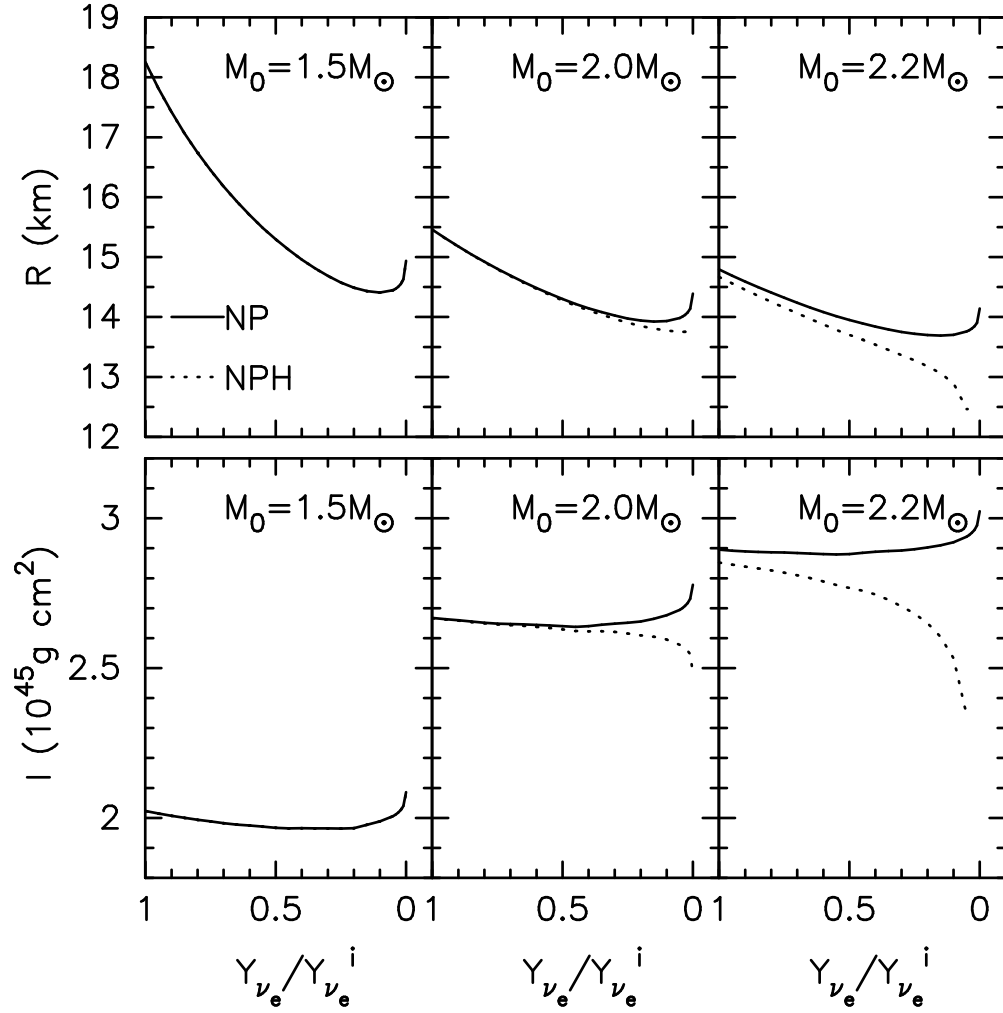


Fig. 9.— The evolution of the stellar radii (upper panels) and the momenta of inertia (lower panels) with the escape of the neutrinos at the different fixed rest masses  $M_0 = 1.5, 2.0, 2.2M_\odot$ . Dotted lines are the results for the PNS with hyperons and solid lines the PNS without hyperons. The initial spin is taken to be  $\Omega = 4000 \text{ s}^{-1}$ .

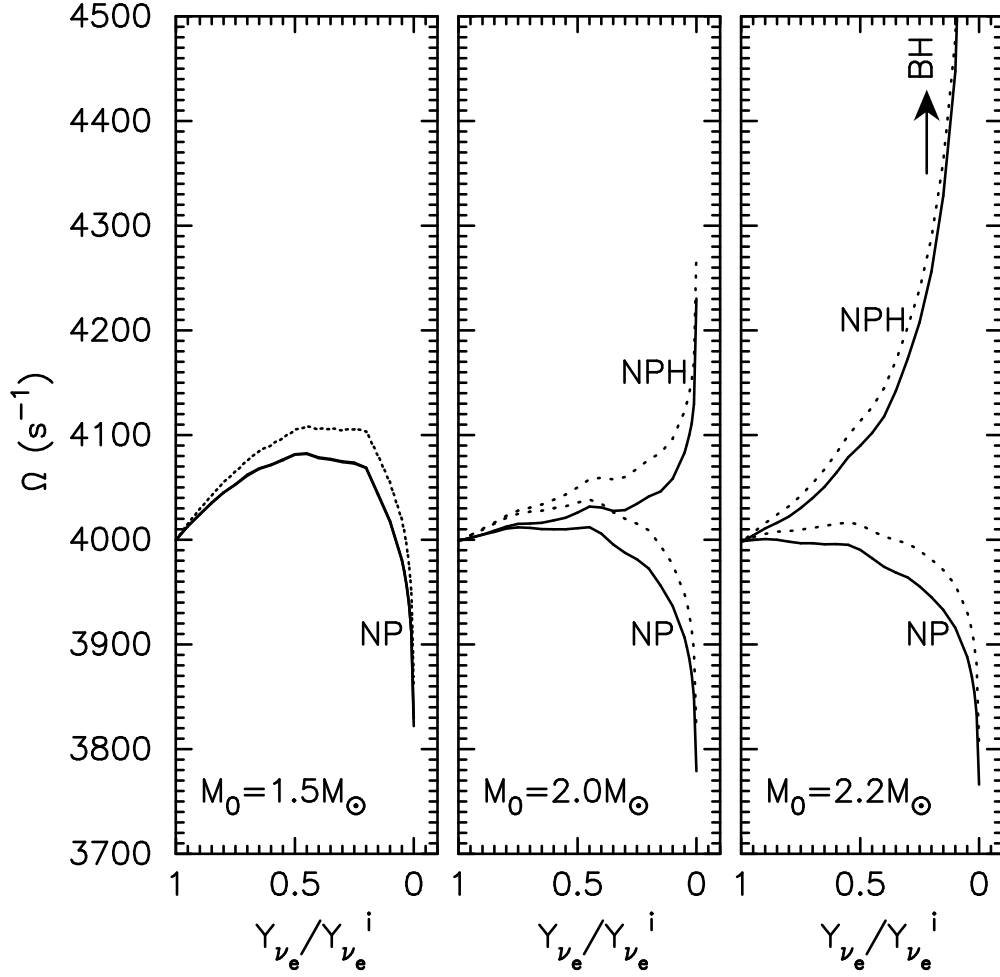


Fig. 10.— The evolution of the rotation frequency of a PNS with hyperons or not at the different fixed rest masses of the star,  $M_0 = 1.5, 2.0, 2.2M_\odot$ . The dotted lines represent the corresponding results for the cases in which the stellar angular momentum carried away by the escaped neutrinos is ignored.

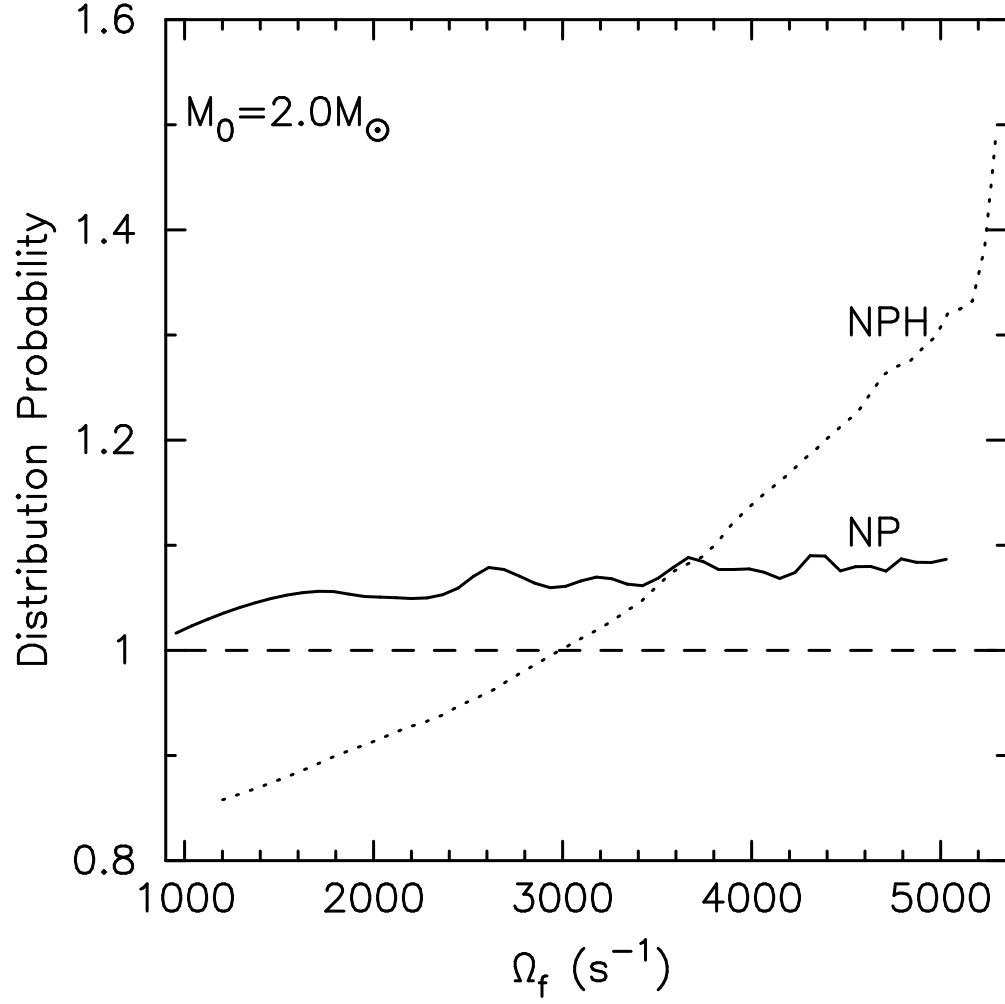


Fig. 11.— The distribution probability (arbitrary units) of the rotation frequencies of the PNSs whose rest mass is  $2.0M_{\odot}$  at the end of the Kelvin-Helmholtz epoch. The dashed line represents the assumed uniform distribution of the initial spin periods.

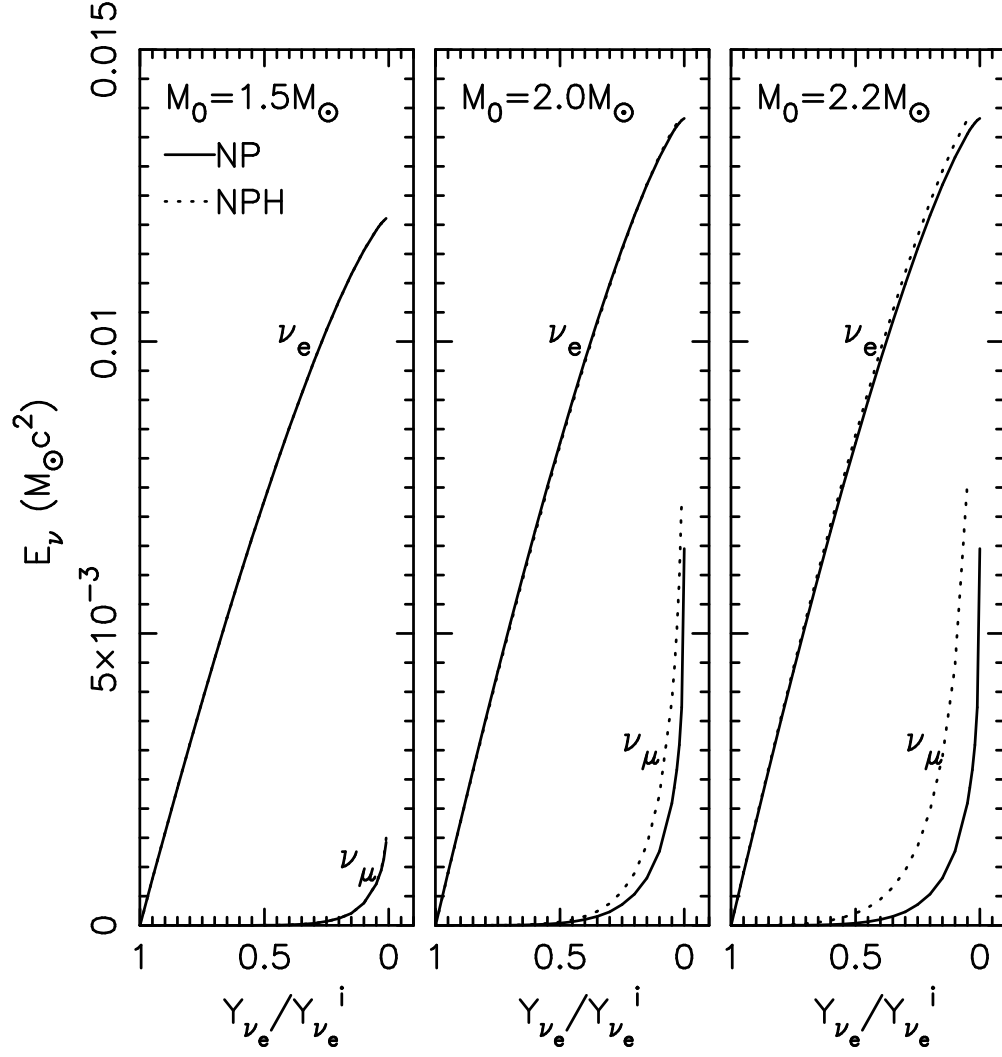


Fig. 12.— The total neutrino energy radiating from the PNS as a function of  $Y_{\nu_e}/Y_{\nu_e}^i$ . The symbol of the lines are the same as Fig. 10.

the neutrinos escape. This characteristic phenomenon is common among them.

In this work, the effect of the temperature is ignored. Certainly regardless of the interior composition, heat introduces another energy source which would make the EOS stiffer than in the zero temperature case. The effect of the cooling of the PNS on the evolution of the PNS could be predicted. However, since the change of the chemical equilibrium among the interior particles dominates the change of the EOS, the cooling of the PNS could not change the results we obtain qualitatively.

In principle, the rotation period of a PNS could be observed by a ground-based gravitational radiation detector, such as LIGO. Fryer et al. (2002) examine several avenues for gravitational wave emission from core collapse. If the core forms a bar or breaks in two, the analysis that we have presented here is inapplicable because we have assumed that the core remains axisymmetric (Eq. 18). Furthermore, the third mode that they considered is the ringdown of the black hole; in this case, the protoneutron-star stage is no longer visible. However, they also have estimated the role that  $r$ -modes may play in gravitational wave generation (Ho & Lai 2000). The frequency of the observed gravitational radiation reflects the spin frequency of the protoneutron star, so the waveform would reveal the internal structure of the protoneutron star as long as fallback did not strongly affect the spin of the core during the Kelvin-Helmholtz epoch. It is unclear whether the  $r$ -modes will have a chance to grow during this early epoch (Fryer et al. 2002), but if they do LIGO-II could detect gravitational radiation from supernovae within 10 Mpc.

As estimated by Eq. 19, a huge energy ( $10^{52}$  ergs) is released in the form of high energy neutrinos during the Kelvin-Helmholtz epoch. If the neutrino flux from the PNS is modulated with the stellar rotation, a neutrino telescope might observe temporal structure at the stellar period, which could provide strict constraints on models of dense matter. The typical energy of the emitted neutrinos is a few MeV (Arnett et al. 1989). Twenty neutrinos were detected from SN1987A (Hirata et al. 1987; Bionta et al. 1987) over about a ten-second interval. Currently, the total sensitivity of detectors sensitive to supernova neutrinos is thirty times larger than in 1987, so one would expect to detect about 15,000 neutrinos from a galactic supernova. Ransom et al. (2002) give straightforward formulae to estimate the minimum pulsed fraction detectable with a given certainty from a sample of arrival times. If we assume that the spin frequency of the PNS lies between zero and 1500 Hz and that the spin may vary by 200 Hz during the ten-second duration of the neutrino burst, a blind search for the spin frequency and its evolution would require about  $3 \times 10^7$  trials. If one wants to detect a signal with a false alarm probability of  $P_0$ , the minimum sinusoidal pulsed fraction that one could detect is

$$f_p = 2 \left[ \frac{\ln(N_{\text{trial}}/P_0) - 1}{N} \right]^{1/2} = 0.08 \quad (20)$$

for a false alarm probability of  $10^{-3}$  and 15,000 detected neutrinos. Because the expected change in frequency is small compared to the expected spin frequency, an unaccelerated search only does marginally better with a minimum detectable pulsed fraction of 0.06. Although these pulsed fractions are several times larger than required for pulsar kicks (*e.g.* Spruit & Phinney 1998; Arras & Lai 1999), Earthbound neutrino detectors are most sensitive to neutrinos in the Wien tail of the thermal distribution where the pulsed fraction will be larger than the momentum anisotropy.

A third observational probe of these models is the distribution of initial periods of neutron stars. This may be obtained from the distribution of current spin periods of radio pulsars along with an independent estimate of the ages of the neutron stars. One must assume that only magnetic dipole radiation has contributed to the spin down, and furthermore that the standard model for magnetic dipole radiation is correct (Kaspi & Helfand 2002). If gravitational radiation is important, then such estimates of the initial spin distribution probe the gravitational radiation epoch (see Owen et al. 1998; Ho & Lai 2000; Watts & Andersson 2002; Arras et al. 2002, for a few viewpoints) rather than the protoneutron-star epoch discussed here. Only a few neutron stars have a good estimates of their initial periods, which are typically an order of magnitude longer than the Kepler period. If the emission of gravitational radiation is not important to the spin evolution of neutron stars, this would argue against a skewed distribution of neutron-star initial spins; however, so few neutron stars have estimates of their initial periods, and the contribution of gravitational radiations is uncertain, it is premature to make any definite conclusions.

The most spectacular manifestation of the rotational evolution of a protoneutron star would be the formation and subsequent collapse of a metastable stellar core. How the core collapses into a black hole and the observable consequences of that collapse are beyond the scope of this paper. We will examine the process in a subsequent paper. For a protoneutron star that rotates rapidly, an important issue is whether the entire protoneutron star can collapse on a dynamical time or portions of the star cannot fall directly into the black hole and form an accretion disk which evolves on a viscous timescale. This could provide a detailed model of the central engines of collapsars, a successful explanation of gamma-ray bursts (MacFadyen et al. 2001).

We have studied the structure of rapidly rotating axisymmetric protoneutron stars using a fully general relativistic treatment of the stellar structure and relativistic mean-field theory to model the equation of state of dense matter. We have contrasted the spin evolution of normal protoneutron stars with hyperonic protoneutron stars. In general the evolution protoneutron stars with other exotic species will be similar to that of hyperonic neutron stars. We have found that hyperonic protoneutron stars can be metastable; that is, the maximum



mass of a stable hyperonic protoneutron star decreases as the neutrinos escape. Both normal and hyperonic protoneutron stars initially spin up as neutrinos escape the outer layers of the protoneutron star and the low-density region shrinks. As neutrinos begin to escape the core of a hyperonic protoneutron star, the core continues to spin up. The metastable protoneutron star continues to spin up as it begins to collapse to a black hole. This contrasts with behavior of a normal protoneutron star. As neutrinos stream out the core of a normal protoneutron star, the equation of state stiffens, the core expands and spins down. This spin evolution leaves a signature on both the neutrino emission and gravitational radiation from the stellar collapse that might be observable from nearby supernovae. Finally, if the processes leading to the formation of hyperonic and normal protoneutron stars are similar, we would expect that the hyperonic neutron stars initially to spin faster than normal neutron stars.

We would like to thank the discussions with Prof. Ramesh Narayan, Prof. K.S. Cheng, Prof. J.L. Zhang, Dr. Scott Ransom and Dr. John Bahcall. Y.F.Y acknowledges the hospitality of Harvard-Smithsonian Center for Astrophysics. Y.F.Y is partially supported by the Special Funds for Major State Research Projects, and the National Natural Science Foundation (10233030). Support for J.S.H. was provided by the National Aeronautics and Space Administration through Chandra Postdoctoral Fellowship Award Number PF0-10015 issued by the Chandra X-ray Observatory Center, which is operated by the Smithsonian Astrophysical Observatory for and on behalf of NASA under contract NAS8-39073.

## REFERENCES

- Akiyama, S., Wheeler, J. C., Meier, D. L., & Lichtenstadt, I. 2003, *ApJ*, 584, 954
- Arnett, W. D., Bahcall, J. N., Kirshner, R. P., & Woosley, S. E. 1989, *ARA&A*, 27, 629
- Arras, P., Flanagan, E. E., Morsink, S. M., rin Schenk, A. K., Teukolsky, S. A., & Wasserman, I. 2002, *ApJ*, accepted (astro-ph/0202345)
- Arras, P. & Lai, D. 1999, *ApJ*, 519, 745
- Bionta, R. M., Blewitt, G., Bratton, C. B., Casper e, D., & Ciocio, A. 1987, *Physical Review Letters*, 58, 1494
- Boguta, J. & Bodmer, A. R. 1977, *Nuclear Physics A*, 292, 413
- Bombaci, I., Prakash, M., Prakash, M., Ellis, P. J., Lattimer, J. M., & Brown, G. E. 1995, *Nuclear Physics A*, 583, 623

- Burrows, A. 2000, *Nature*, 403, 727
- Burrows, A., Hayes, J., & Fryxell, B. A. 1995, *ApJ*, 450, 830
- Cheng, K. S., Yuan, Y. F., & Zhang, J. L. 2002, *ApJ*, 564, 909
- Chin, S. A. 1977, *Ann. of Phys.*, 108, 301
- Chubarian, E., Grigorian, H., Poghosyan, G., & Blaschke, D. 2000, *A&A*, 357, 968
- Fryer, C. L. & Heger, A. 2000, *ApJ*, 541, 1033
- Fryer, C. L., Holz, D. E., & Hughes, S. A. 2002, *ApJ*, 565, 430
- Glendenning, N. K. 1992, *Phys. Rev. D*, 46, 4161
- Glendenning, N. K. 2000, *Compact Stars, Nuclear Physics, Particle Physics, and General Relativity* (New York: Springer)
- Glendenning, N. K. & Moszkowski, S. A. 1991, *Physical Review Letters*, 67, 2414
- Glendenning, N. K., Pei, S., & Weber, F. 1997, *Physical Review Letters*, 79, 1603
- Goussard, J. O., Haensel, P., & Zdunik, J. L. 1997, *A&A*, 321, 822
- Goussard, J.-O., Haensel, P., & Zdunik, J. L. 1998, *A&A*, 330, 1005
- Hartle, J. B. 1967, *ApJ*, 150, 1005
- Hartle, J. B. & Thorne, K. S. 1968, *ApJ*, 153, 807
- Hashimoto, M., Oyamatsu, K., & Eriguchi, Y. 1994, *ApJ*, 436, 257
- Hirata, K., Kajita, T., Koshiha, M., Nakahata, M., & Oyama, Y. 1987, *Physical Review Letters*, 58, 1490
- Ho, W. C. G. & Lai, D. 2000, *ApJ*, 543, 386
- Janka, H.-T., Buras, R., Kifonidis, K., Plewa, T., & Rampp, M. 2003, in *From Twilight to Highlight: The Physics of Supernovae. Proceedings of the ESO/MPA/MPE Workshop held in Garching, Germany, 29-31 July 2002*, p. 39., 39–+
- Kaspi, V. M. & Helfand, D. J. 2002, in *ASP Conf. Ser. 271: Neutron Stars in Supernova Remnants*, 3, astro-ph/0201183
- Komatsu, H., Eriguchi, Y., & Hachisu, I. 1989a, *MNRAS*, 237, 355

- . 1989b, MNRAS, 239, 153
- Lorenz, C. P., Ravenhall, D. G., & Pethick, C. J. 1993, Physical Review Letters, 70, 379
- Müller, H. & Serot, B. D. 1996, Nuclear Physics A, 606, 508
- MacFadyen, A. I., Woosley, S. E., & Heger, A. 2001, ApJ, 550, 410
- Owen, B. J., Lindblom, L., Cutler, C., Schutz, B. F., Vecchio, A., & Andersson, N. 1998, Phys. Rev. D, 58, 84020
- Pons, J. A., Miralles, J. A., Prakash, M., & Lattimer, J. M. 2001a, ApJ, 553, 382
- Pons, J. A., Reddy, S., Prakash, M., Lattimer, J. M., & Miralles, J. A. 1999, ApJ, 513, 780
- Pons, J. A., Steiner, A. W., Prakash, M., & Lattimer, J. M. 2001b, Physical Review Letters, 86, 5223
- Prakash, M., Bombaci, I., Prakash, M., Ellis, P. J., Lattimer, J. M., & Knorren, R. 1997, Phys. Rep., 280, 1
- Prakash, M., Cooke, J. R., & Lattimer, J. M. 1995, Phys. Rev. D, 52, 661
- Rampp, M. & Janka, H.-T. 2002, A&A, 396, 361
- Ransom, S. M., Eikenberry, S. S., & Middleditch, J. 2002, AJ, 124, 1788
- Reddy, S., Prakash, M., & Lattimer, J. M. 1998, Phys. Rev. D, 58, 13009
- Serot, B. D. 1979, Phys. Lett. B, 86, 146
- Serot, B. D. & Walecka, J. D. 1986, Adv. Nucl. Phys., 16, 1
- Spruit, H. C. & Phinney, E. S. 1998, Nature, 393, 139
- Stergioulas, N. 1998, Living Reviews in Relativity, 1, 8
- Stergioulas, N. & Friedman, J. L. 1995, ApJ, 444, 306
- Strobel, K., Schaab, C., & Weigel, M. K. 1999, A&A, 350, 497
- Sumiyoshi, K., Ibáñez, J. M., & Romero, J. V. 1999, A&AS, 134, 39
- Takatsuka, T., Nishizaki, S., & Hiura, J. 1994, Progress of Theoretical Physics, 92, 779
- Thompson, C. & Duncan, R. C. 1993, ApJ, 408, 194

- Vidaña, I., Bombaci, I., Polls, A., & Ramos, A. 2003, *A&A*, 399, 687
- Walecka, J. D. 1974, *Ann. of Phys.*, 83, 491
- Watts, A. L. & Andersson, N. 2002, *MNRAS*, 333, 943
- Weber, F. & Glendenning, N. K. 1992, *ApJ*, 390, 541
- Yuan, Y. F. & Zhang, J. L. 1999, *ApJ*, 525, 950